HSLA-100 Steels: Influence of Aging Heat Treatment on Microstructure and Properties

M. Mujahid, A.K. Lis, C.I. Garcia, and A.J. DeArdo

(Submitted 10 September 1997; in revised form 10 November 1997)

The structural steels used in critical construction applications have traditionally been heat-treated low-alloy steels. These normalized and/or quenched and tempered steels derive strength from their carbon contents. Carbon is a very efficient and cost-effective element for increasing strength in ferrite-pearlite or tempered martensitic structures, but it is associated with poor notch toughness. Furthermore, it is well known that both the overall weldability and weldment toughness are inversely related to the carbon equivalent values, especially at high carbon contents. The stringent control needed for the welding of these traditional steels is one of the major causes of high fabrication costs.

In order to reduce fabrication cost while simultaneously improving the quality of structural steels, a new family of high-strength low-alloy steels with copper additions (HSLA-100) has been developed. The alloy design philosophy of the new steels includes a reduction in the carbon content, which improves toughness and weldability.

Keywords aging, copper precipitation, heat treatment, HSLA steels, mechanical properties

1. Introduction

For several decades ferrite-pearlite and quenched and tempered (Q&T) steels have been the only plate steels available for high-strength structural applications. Ferrite-pearlite steels, also called high tensile strength (HTS) steels, were the first to be used for applications such as shipbuilding. These are C-Mn steels of moderate strength (350 MPa) and essentially consist of a mixture of large-grained ferrite and coarse pearlite. Thus the strength in these steels is obtained through pearlite strengthening by the addition of carbon up to 0.2% (Ref 1). In the 1960s, Q&T steels were developed to improve the performance of structural members in naval applications. These are used in the tempered martensite condition and exhibit high strength (560 to 690 MPa). The Q&T steels also rely on carbon for strength, and they contain alloying elements required for adequate hardenability. Both the HTS and Q&T steels exhibit adequate base-plate properties for their intended end use. However, HY steels suffer from poor weldability, which is caused by both the high carbon content and high carbon equivalent values (i.e., high hardenability levels).

After the failure of welded structures occurred by brittle fracture, it was recognized that impact or fracture toughness was essential. The need for a low-impact transition temperature became apparent, because the structures of the traditional steels are highly sensitive to hydrogen-induced cracking of heat-affected zones (HAZs) after welding. The presence of hydrogen, even in very small amounts, can cause cold cracking. Hence, to avoid hydrogen diffusion into the welded zones and HAZs, the parts to be welded should be preheated for a long time and the welding process itself requires controlled interpass temperatures and heat input limitations (Ref 2, 3). Furthermore, the presence of high carbon contents and large amounts of alloying elements required to obtain the proper hardenability and strength also leads to very high carbon equivalent values.

It is now well known that both the weldability and weldment toughness are inversely related to the carbon equivalent value, especially at high carbon contents. For this reason, the weldability of Q&T steels has been, and continues to be, rather

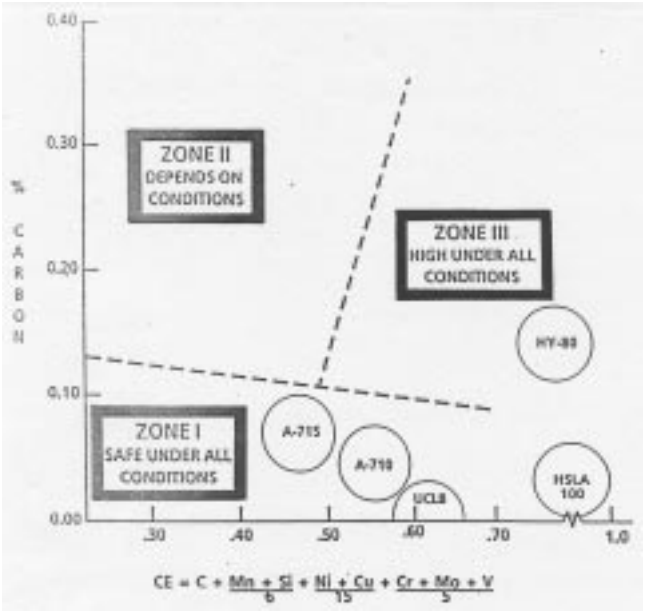

Fig. 1 Susceptibility to heat-affected zone cracking. The carbon equivalent is the same as in Ref 4.

M. Mujahid, Faculty of Metallurgy and Materials Engineering, GIK Institute of Engineering Sciences & Technology, Topi, NWFP-23460, Pakistan; and **A.K. Lis, C.I. Garcia,** and **A.J. DeArdo,** Basic Metals Processing Research Institute, Department of Materials Science and Engineering, University of Pittsburgh, PA 15261, USA.

poor (Fig. 1). Thus, a potentially more important consideration in the alloy design of plate steels may be the toughness of the HAZ in multipass welding operations. A recent investigation revealed the importance of HAZ composition and microstructure on HAZ toughness (Ref 5). This study showed the critical importance of the amount and size of martensite-austenite islands on the HAZ toughness. Hence, plate steels that have high carbon and alloy contents, which are required for high strength, have the potential for low HAZ toughness. Figure 1 suggests the critical importance of low carbon contents in improving the weldability and weldment toughness in plate steels.

Thus, the major developments in the plate steel area have been stimulated by the demand for (Ref 6):

- Higher yield strength, for greater load-bearing capacity by lighter sections
- High resistance to brittle fracture, as well as low transition temperature
- A high degree of weldability

These requirements have led to the development of a series of new low-carbon steels. These new approaches generally rely on a low to very low carbon content, sufficient alloying to obtain the desired transformation temperature, and microalloying and thermomechanical processing for microstructural refinement. The strengthening mechanisms in the new steels are largely independent of carbon content, unlike the older ferrite-pearlite or martensitic plate steels. Furthermore, such steels have a very fine grain size and can exhibit very good strength and toughness in the as-hot-rolled condition (Ref 7).

The present study summarizes some of the results of the research work carried out on the development of HSLA-100 steels for structural applications. It discusses the phase changes that take place during different stages of aging of 25 mm thick hot-rolled HSLA-100 plates.

2. Experimental Procedures

The chemical compositions (in wt%) of the two steels used in this study are shown in Table 1. The as-received material was in the form of control-rolled plates of dimensions 100 × 25 × length mm. The heat treatment was employed after cutting the plates into pieces of dimensions 102 × 25 × 25 mm. the heat treatment consisted of austenitizing at 900 °C for 1 h followed by a water quench. The plate pieces were then aged for 1 h in the temperature range of 450 to 730 °C and then air cooled to room temperature.

Table 1 Chemical compositions of the plate steels (wt%)

	Composition, wt%											
Steel	**C**	**Mn**	**Ni**	**Cr**	**Cu**	**Mo**	**Nb**	**Si**	**Al**	**N**	**P**	**S**
B	0.057	0.99	3.42	0.67	1.66	0.60	0.036	0.38	0.024	0.011	0.010	0.001
C	0.036	0.91	3.59	0.59	1.60	0.59	0.025	0.24	0.022	0.010	0.008	0.005

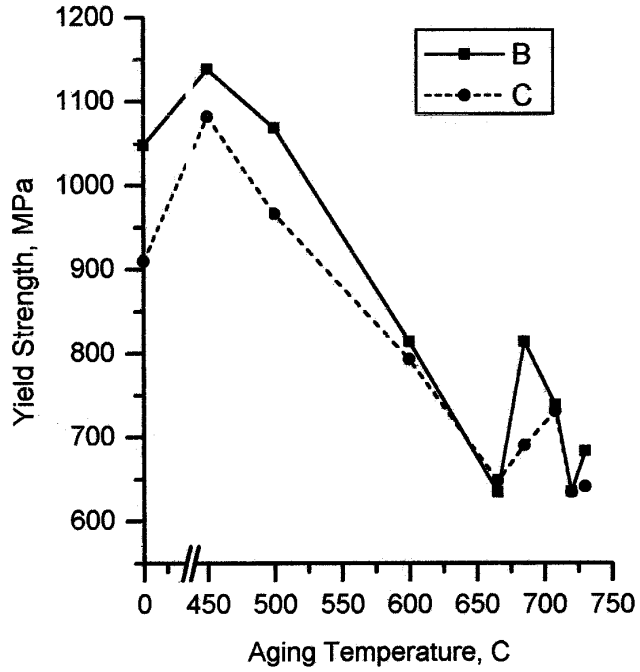

Fig. 2 Variation of room-temperature strength with aging temperature of as-quenched HSLA-100 steels

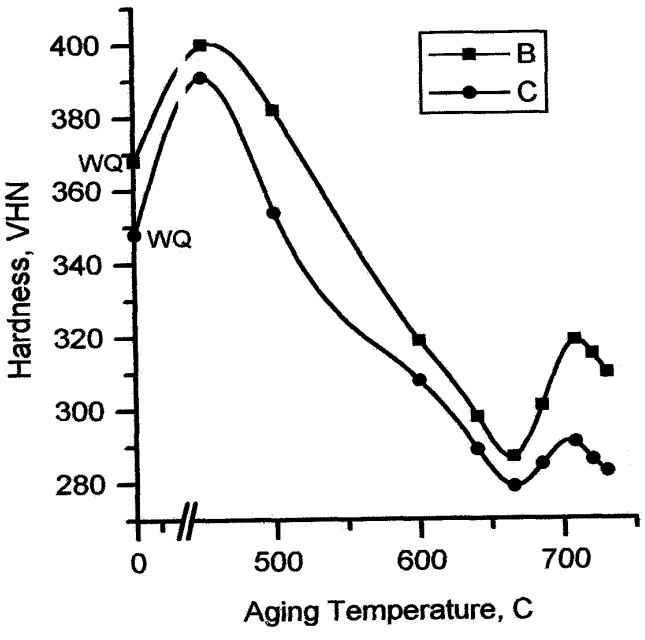

Fig. 3 Variation of room-temperature hardness with aging temperature of as-quenched HSLA-100 steels

The mechanical properties, such as hardness, strength, and impact toughness, were determined in all conditions. The geometries of the tensile and the Charpy impact test specimens conformed to ASTM standard A 370. The specimens were cut transverse to the rolling direction while the notch of the Charpy specimens was perpendicular to the rolling plane (T-L orientation).

Table 2 Mechanical properties of steel B in all conditions

Sample No.	Aging temperature, °C	Hardness, VHN	Yield strength, MPa	Ultimate tensile strength, MPa	Elongation, %	Toughness, J, at: +25 °C	–18 °C	–85 °C	–100 °C
BW	WQ	368	1048	1124	16	97	102	57	45
B1	450	400	1038	1158	16.5	27	15	7	7
B2	500	382	1068	1103	17	65	39	24	20
B3	600	319	814	848	23.5	108	104	58	46
B4	640	298	848	868	22	160	92	96	64
B5	665	287	634	813	24	134	123	112	110
B6	685	301	814	972	19	138	138	115	84
B7	708	319	738	993	19.5	119	116	104	89
B8	720	315	635	875	21.5	115	114	103	92
B9	730	310	683	979	22	146	145	125	108

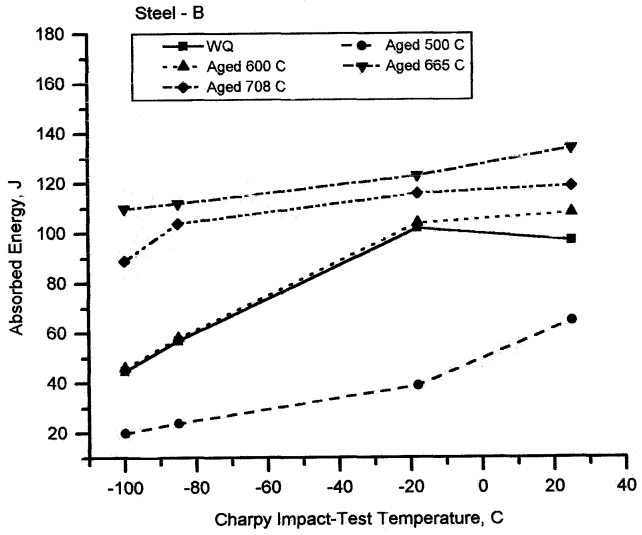

Fig. 4 The influence of test temperature and aging condition on impact toughness of steel B

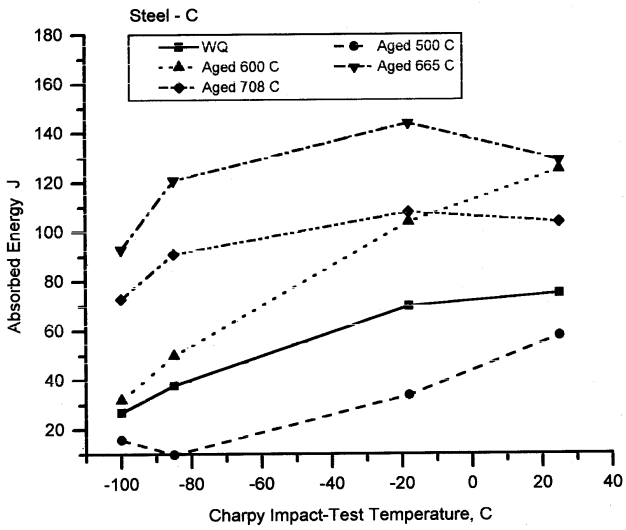

Fig. 5 The influence of test temperature and aging condition on impact toughness of steel C

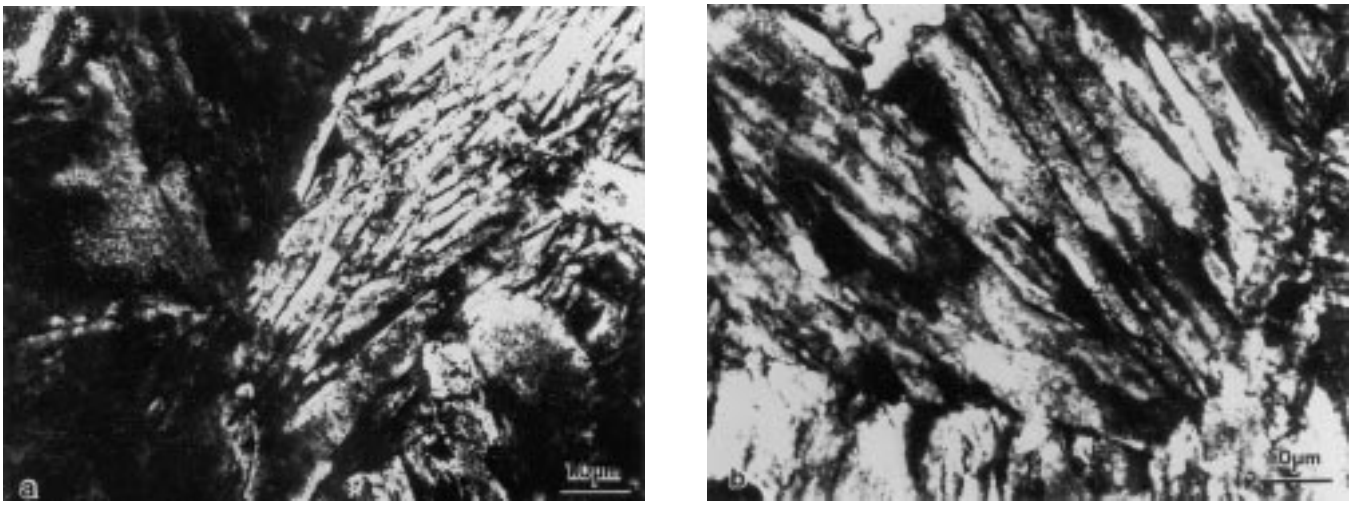

Fig. 6 Bright-field TEM micrographs showing lath martensite in the steels that were water quenched after austenitizing at 900 °C for 1 h. (a) Steel B. (b) Steel C

The overall microstructure of the steels in all conditions of heat treatment was examined using JEOL 200CX/2000FX transmission electron microscopes, carbon extraction replicas, and thin foil specimens. The jet polishing of thin foils was done using a solution of 33% perchloric acid in ethanol at –50 °C. The different phases were analyzed, to determine the dominant constituents, with the help of the energy-dispersive spectrometer available in the JEOL 2000FX instrument.

3. Results

3.1 Mechanical Properties

Mechanical properties of the steels in all conditions are shown in Tables 2 and 3. Figure 2 shows aging curves plotted between yield strength and aging temperature for both the steel plates. A similar trend was also observed in the hardness of the two steels when plotted against aging temperature (Fig. 3). The aging behavior of these steels can be separated into four distinct stages. Stage I is associated with the highest strength level at 450 °C. Stage II (450 to 665 °C) is characterized by a continuous decrease in strength. Stage III is associated with a secondary strengthening, observed around 708 °C, while stage IV occurs above 708 °C with a decrease in strength again.

The results shown in Fig. 4 and 5 show the impact energy of the steels as a function of test temperature. The results indicate that the steels aged at about 450 to 500 °C exhibit very low resistance to brittle fracture. However, the toughness improved extraordinarily as the aging temperature was increased above 600 °C. The best combination of yield strength and toughness was obtained when the steels were aged at 640 °C.

3.2 Microstructural Characterization

The steels in the water-quenched (WQ) condition were essentially composed of low-carbon lath martensite and small amounts of retained austenite. The martensite laths were observed to be several microns long and approximately 0.5 μm wide (Fig. 6). The laths were mostly separated by low-angle boundaries and were highly dislocated. A very small amount of retained austenite was observed between the martensite laths (Fig. 7).

In the first stage of aging (at about 450 °C), the steels still exhibited a lath martensite structure with a dislocation density apparently similar to that observed in the WQ condition. In addition, moiré patterns were observed in some regions, suggesting the presence of fine copper clusters (Fig. 8). The carbon

Table 3 Mechanical properties of steel C in all conditions

Sample No.	Aging temperature, °C	Hardness, VHN	Yield strength, MPa	Ultimate tensile strength, MPa	Elongation, %	Toughness, J, at: +25 °C	–18 °C	–85 °C	–100 °C
CW	WQ	348	910	1020	16	75	70	38	27
C1	450	391	1082	1103	19	31	18	12	12
C2	500	354	966	1048	19.5	58	34	10	16
C3	600	308	793	855	23	125	104	50	32
C4	640	289	772	800	26	128	133	95	66
C5	665	279	648	820	23	129	144	121	93
C6	685	285	690	862	22	122	108	98	81
C7	708	291	731	882	22	104	108	91	73
C8	720	286	634	882	22	119	122	104	98
C9	730	283	641	875	23	119	118	110	93

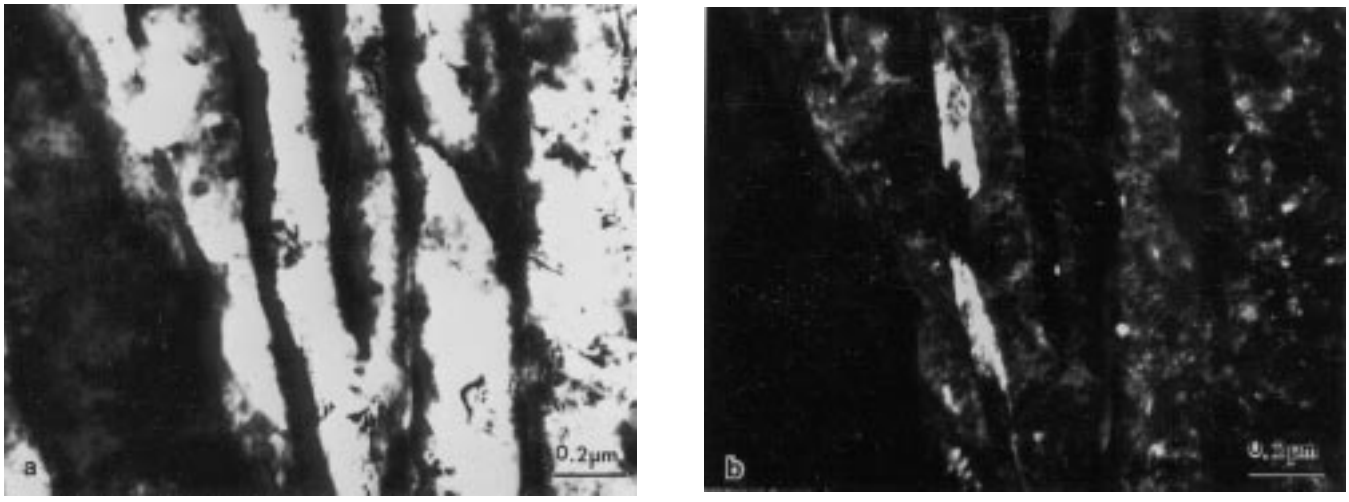

Fig. 7 TEM micrograph of steel C in WQ conditions showing the presence of retained austenite at the lath boundaries. (a) Bright-field image. (b) Dark-field image

extraction replicas revealed that Nb(C, N) precipitates were also present (Fig. 9). These Nb(C, N) particles were probably formed during thermomechanical processing of the steels. The precipitates were spherical in shape and were observed to have a diameter ranging from 100 to 300 Å.

During stage II of aging, a continuous process of recovery and, later, recrystallization of the matrix occurred. In the initial phase of stage II (at 500 °C), copper precipitates were observed to be spherical in shape with diameters less than 100 Å (Fig. 10). The selected area diffraction patterns from the copper precipitates revealed that they had a face-centered cubic (fcc) crystal structure and that the lattice parameter was 3.58 ± 0.04 Å.

At the aging temperature of 640 °C, nucleation of a new phase was observed at some of the prior lath boundaries (Fig. 11). The new phase was assumed to be austenite, based on the fcc crystal structure and the measured lattice parameter ($a_0 = 3.6 \pm 0.02$ Å). The selected area diffraction pattern from this new austenite is shown in Fig. 10(c). Further investigations carried out using scanning transmission electron microscopy with energy-dispersive spectrometry revealed that the new austenite was rich in alloying elements such as nickel, copper, manganese, and chromium (Fig. 12). As the aging temperature was increased, the volume fraction of the new austenite also increased. Most of the new austenite that formed on heating up to 665 °C was observed to be retained even after air cooling of the steel from the aging temperature (Fig. 13).

In stage III of aging, the matrix was apparently fully recovered but not completely recrystallized. Dislocations were still present and were seen to be interacting with large rodlike copper particles. The volume fraction of the new austenite was observed to increase significantly if the steel was aged for 1 h above 665 °C. The new austenite transformed predominantly to highly dislocated lath martensite and retained new austenite on cooling from higher aging temperatures (Fig. 14), although in some regions of steel B, microtwins were also observed (Fig. 15) in the martensite laths.

In stage IV of aging, the new austenite was observed to have transformed to softer bainitic structures upon cooling. Also, the number of large copper precipitates was greatly reduced, as a very large amount of new austenite was found in this stage. Figure 16 shows a schematic illustration of the aging behavior of HSLA-100 steel and the variation of microstructural constituents with aging temperature.

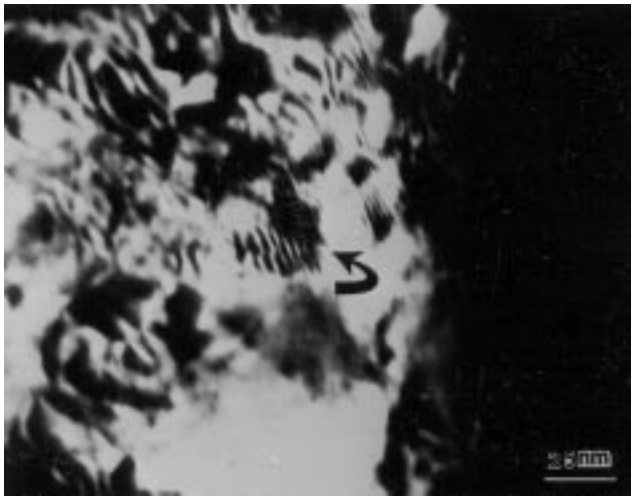

Fig. 8 Moiré patterns indicating the presence of copper clusters in steel C aged at 450 °C, thin foil

4. Discussion

4.1 Influence of Processing on Microstructure

As-Quenched Condition. According to the Fe-Cu phase diagram (Ref 8), the maximum solubility of copper in austenite is 2.1 wt% at 850 °C but decreases with decreasing temperature. Thus, the austenitizing temperature used in the present study seems to be high enough to have all the copper in solution. On quenching from this temperature, a supersaturated solid solution is obtained with all of the copper in solution in martensite. It is known (Ref 9) that copper slightly lowers the allotropic and M_s (martensite start) temperatures, the extent of

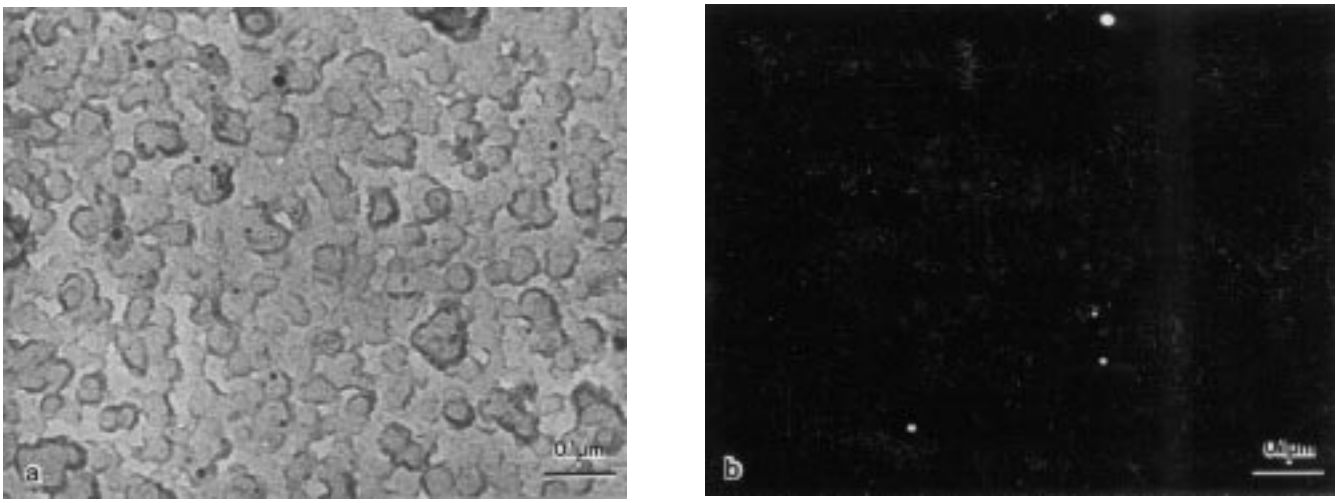

Fig. 9 TEM image of Nb(C, N) precipitates taken with carbon extraction replicas of samples aged at 450 °C. (a) Bright-field image. (b) Dark-field image

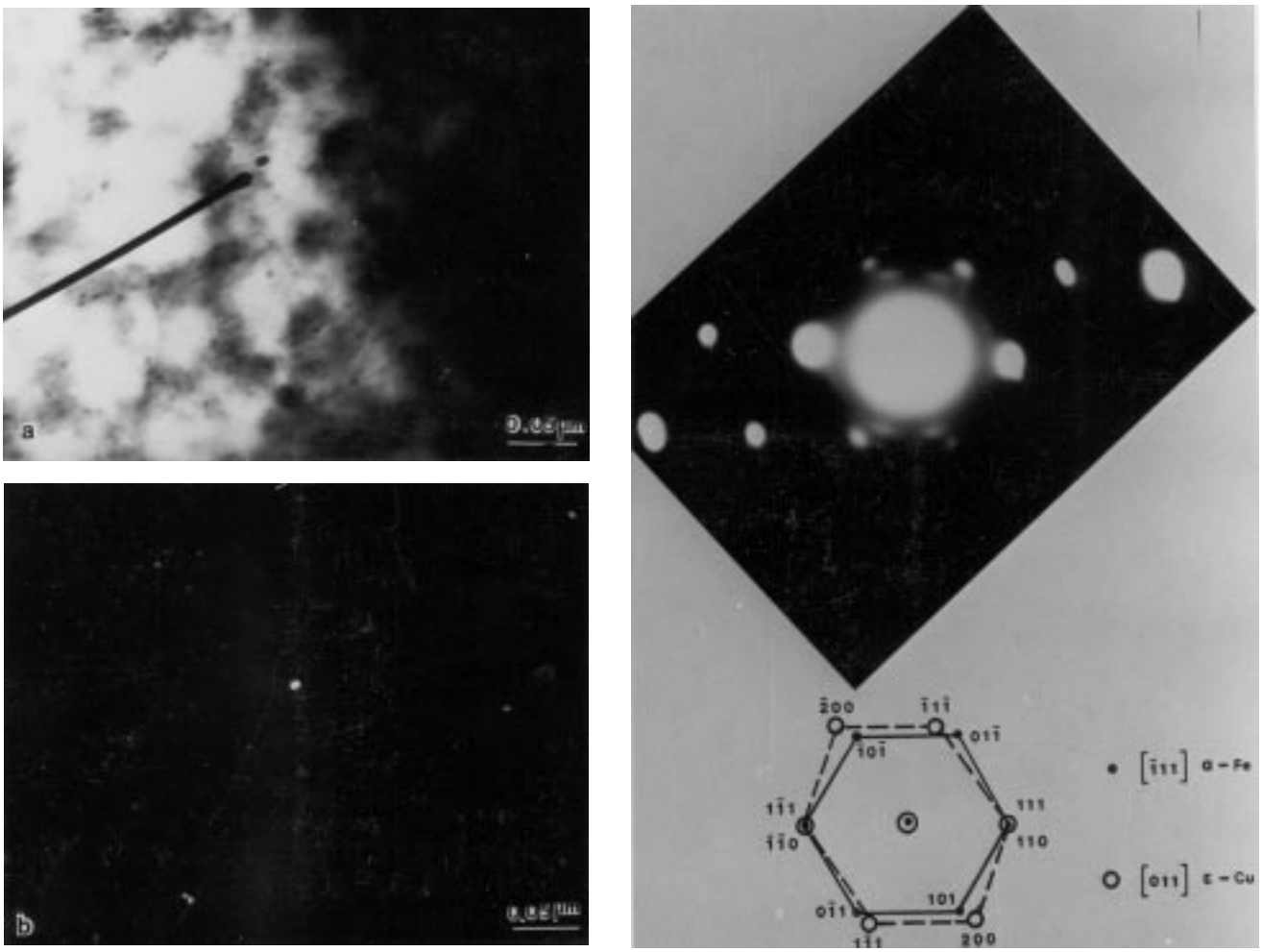

Fig. 10 Thin foil TEM images of copper precipitates of less than 100 Å diameter (sample aged at 500 °C). (a) Bright-field image. (b) Dark-field image. (c) Selected-area diffraction pattern

decrease being proportional to the copper content. In addition, other solute elements present in the steel (especially nickel) are also considered to be austenite-stabilizing elements. Therefore, the decomposition of austenite in the present steels will be delayed. Because of the very low carbon contents of these steels, only a highly dislocated lath martensite structure was observed. It is well known (Ref 10) that twins do not occur extensively in this type of martensite (i.e., in steels with carbon content < 0.5%). As the carbon content of the steels decreases, the tetragonality of the lath martensite also decreases. Thus, the crystal structure of the lath martensite with carbon content below 0.2% is essentially body-centered cubic (bcc).

Influence of Aging on Structure. The steel in the WQ condition consists of an α′-phase (martensite supersaturated with copper), and thus precipitation of ε-phase (copper) and annealing of the matrix occur during aging. Earlier studies (Ref 9) on binary Fe-Cu alloys have shown that the aging process can be described in terms of the formation and growth of coherent bcc copper-rich clusters, the transformation of these to fcc ε-phase particles, and the subsequent growth of these to form rodlike precipitates at high aging temperatures. In the present study, the coherent copper-rich clusters were observed to form in stage I of aging (450 °C). Due to the lack of diffraction and strain contrast from ε-phase, the presence of copper clusters was detected only by moiré patterns. In the same context, Hornbogen (Ref 11-13) suggested that the bcc copper-rich clusters readily transform to fcc copper at a relatively small size and that as a result the strain contrast associated with coherent precipitates is not observed. Field ion microscopy studies (Ref 14, 15) of aged Fe-Cu alloys have shown that these initial clusters have bcc structure and contain significant amounts of iron. In addition, they are coherent with the matrix and have a very small lattice parameter mismatch. In stage I of aging, the matrix still consists of a lath structure with a dislocation density similar to that of the WQ condition.

With the increase of aging temperature (to between 450 and 600 °C), there is a simultaneous as well as continuous process of recovery of martensite laths and coarsening of precipitates. At this stage, spherical ε-Cu precipitates become resolvable in the transmission electron microscope because the diffraction contrast can be obtained. During the coarsening process in stage II, the number and density of copper particles decrease

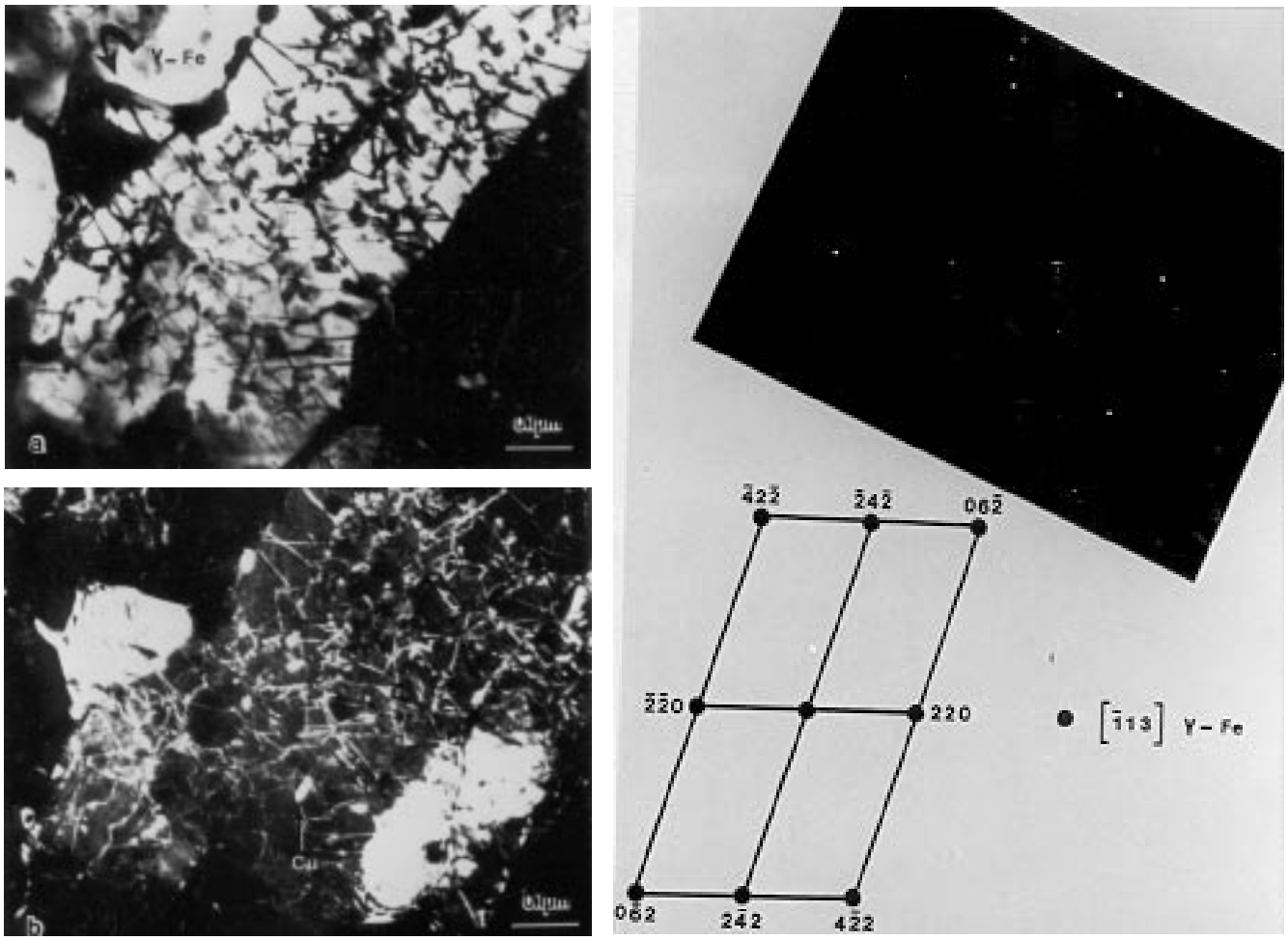

Fig. 11 Nucleation of new austenite at lath boundaries and rod-shaped copper particles, steel C aged at 640 °C. (a) Bright-field image. (b) Dark-field image. (c) Selected-area diffraction pattern

and the average size increases by a ripening process. Further overaging of the steels occurs when the spherical ε-Cu precipitates change their shape to rodlike particles. This is in accordance with the work of Speich and Oriani (Ref 16), who showed that the equilibrium shape of the particles is that of rods with hemispherical caps, due to a large anisotropy in the Cu/α-Fe interfacial free energy. This anisotropy in turn is due to the poor atomic fit at the ends of the particles, in contrast with the excellent atomic fit along the cylindrical sides.

At temperatures above 600 °C, the lath structure is partially recovered and has a moderate dislocation density. In addition, recrystallization of ferrite starts in some areas. Formation of new austenite occurs in the steels when they are aged at about 640 °C. This is because the Ac_1 temperature for the present steel is around 635 °C, which is in good agreement with the results of Ricks et al. (Ref 17), who were working on Fe-Ni-Cu alloys. The new austenite was observed to form within the prior-tempered-martensite matrix at the interlath as well as at high-angle boundaries, because these are preferred sites for heterogeneous nucleation. The growth of this new austenite was both perpendicular and parallel to the grain boundaries. As in earlier studies (Ref 18), the growth of austenite occurred at significant rates in both directions above 665 °C, but the principal growth direction was parallel to the martensitic ferrite laths or at the prior-austenite grain boundaries. This asymmetry in growth rates can be explained on the basis of the pertinent diffusion coefficients. In diffusion-controlled growth models (Ref 19-20), the growth rate is usually taken to be proportional to the diffusion coefficient. That is, the growth rate perpendicular to the boundary would be controlled by bulk diffusion coefficient, whereas the growth rate parallel to the boundary would be controlled by a coefficient related to boundary diffusion. Also, it is well recognized (Ref 19-20) that the mass transport occurs most readily by bulk diffusion at high temperatures (>0.7 T_{melt}) and by boundary diffusion at low temperatures. In the early stages of its development, the new austenite was observed to be rich in alloying elements such as nickel, copper, manganese, and chromium (Fig. 12). The solutes apparently reached the growing austenite by diffusion radially inward and also along high-diffusivity paths such as dislocations and boundaries.

The transformation behavior of this newly formed austenite is very important, because it appears to have a strong and direct influence on the final properties. In the initial stages of its formation during aging, austenite becomes rich in solutes (especially nickel and copper) by depleting the matrix, which makes

the austenite highly stable even when the steel is air cooled to room temperature. The austenite in this condition is seen to be free of dislocations, and a precipitate-free zone is observed around it. Other studies (Ref 21, 22) on Fe-Ni alloys have shown that it is primarily the composition of austenite that controls its thermal stability. However, at higher aging temperatures the growth of the newly formed austenite causes the dilution of solutes in the new austenite. The dilution in the amount of solutes causes the new austenite to transform to martensitic or bainitic structures on cooling. Steven et al. (Ref 23) have given the M_s (temperature at which new austenite begins to transform spontaneously to martensite) in terms of the austenite composition:

$$M_s\ (°C) = 561\text{-}474(\%C)\text{-}33(\%Mn)\text{-}17(\%Ni)\text{-}17(\%Cr)$$

The strong dependence of the M_s on the composition of austenite is in accordance with the steel used in this study, where the newly formed austenite remains thermally stable upon cooling when formed at aging temperatures up to 665 °C. This is because the new austenite in this condition has lower volume fraction but is rich in austenite-stabilizing elements. However, when formed during stage III of aging, the new austenite has a larger volume fraction but is low in austenite-stabilizing elements; hence, it transforms to martensite upon cooling. A further increase in aging temperature produces a bainitic structure.

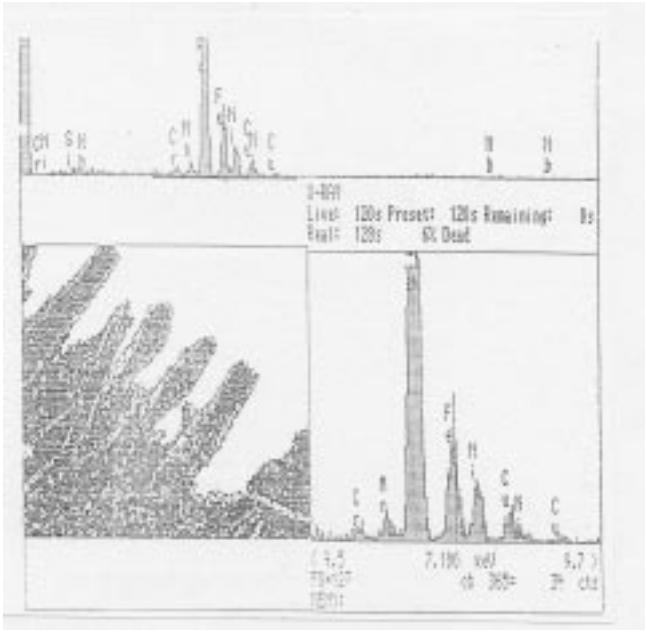

Fig. 12 Qualitative elemental analysis, using scanning transmission electron microscopy with energy-dispersive spectrometry, from newly formed austenite in steel C, showing significant peaks of alloying elements such as nickel, copper, manganese, and chromium

4.2 Influence of Processing on Mechanical Properties

Hardness and Strength. In general, strength is taken as a measure of the resistance to plastic flow. Thus, all strengthening mechanisms apparently reduce the dislocation mobility and increase the stress required to move the dislocations through large distances within the material. The present steels in the WQ condition derive much of their strength from carbon in solution in martensite and from the high dislocation density in the laths of the alloyed martensite. Copper and other alloying elements that are present as substitutional atoms provide relatively small increments in strength.

In stage I of aging, the peak in strength and hardness at 450 °C corresponds to the formation of coherent copper-rich clusters. Field ion microscopy studies (Ref 14, 15) of aged Fe-Cu alloys have suggested that the peak strength observed in the early stages of aging might be due to the fact that the precipitates formed are highly supersaturated Cu-Fe solutions rather than nearly pure copper. In another model, Russell and Brown (Ref 24) have described this strength increase in terms of a modulus interaction theory, i.e., the dislocation cuts the obstacle but the line tension of the dislocation within the obstacle is

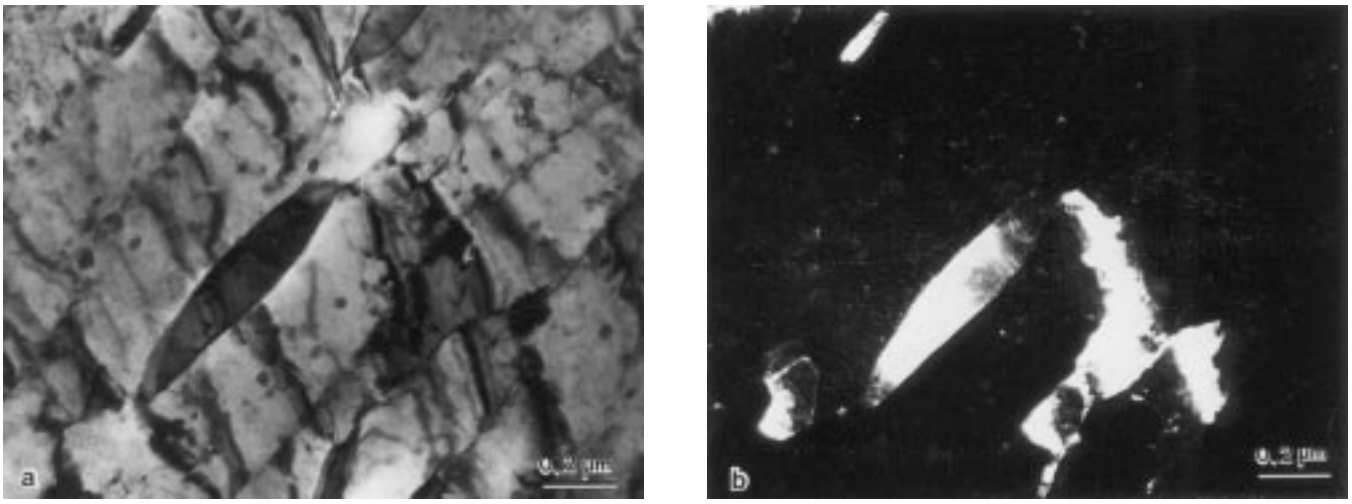

Fig. 13 Thin foil TEM micrograph of steel C aged at 665 °C, showing newly formed austenite at lath boundaries being retained after air cooling. (a) Bright-field image. (b) Dark-field image

reduced; hence, additional work is needed to pull the dislocation out of the cluster.

Transformation of the bcc copper-rich clusters to fcc copper occurs at a relatively small size (at less than 100 Å) and in a temperature range of 450 to 500 °C. At this stage, the strength of the steels is still reasonably high. This can be attributed to the uniform dispersion of very small coherent ε-Cu particles, which interact with a large number of dislocations still present in the lath structure, and to the partially recovered unrecrystallized matrix.

Loss of coherency due to coarsening of copper precipitates and the beginning of the recovery and recrystallization process of the matrix occurs in the early part of stage II. Because of these softening effects, a continuous decrease in strength is observed in the steels. Formation of the new austenite in stage II of aging has not shown any significant effects on strength. However, in stage III, the new austenite transforms to martensite that corresponds to the second strengthening peak observed in the aging curves. Finally, in stage IV, the steels show a bainitic structure and thus a softening trend again follows.

As compared with steel C, the strength levels in steel B were higher under all aging conditions. The secondary strengthening in steel B was also observed to be greater, and the peak was displaced further to higher aging temperatures, compared with steel C. These effects can be attributed to the presence of higher carbon contents in steel B, which would produce harder martensite. The observed microtwins in the transformation product of newly formed austenite in steel B (during stage III of aging) supports the above argument.

Toughness. The results indicate that the steels possess a reasonable amount of notch toughness in the WQ condition. This is because the present steels consist of low-carbon lath martensite in this condition. It has already been established

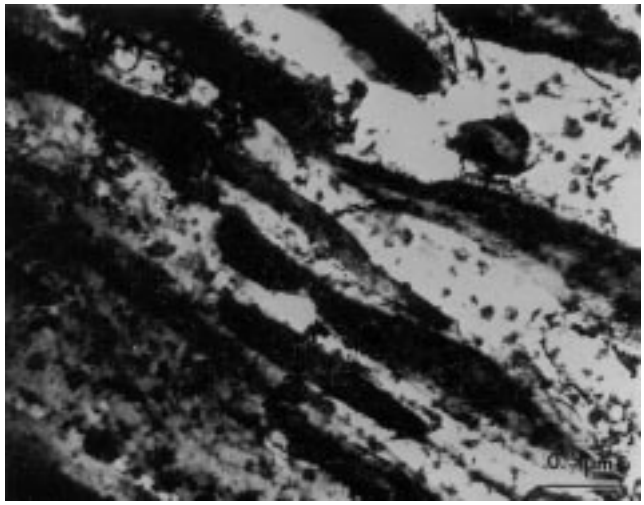

Fig. 14 Thin foil TEM image of steel C (aged at 708 °C) showing new austenite transformed to dislocated lath martensite

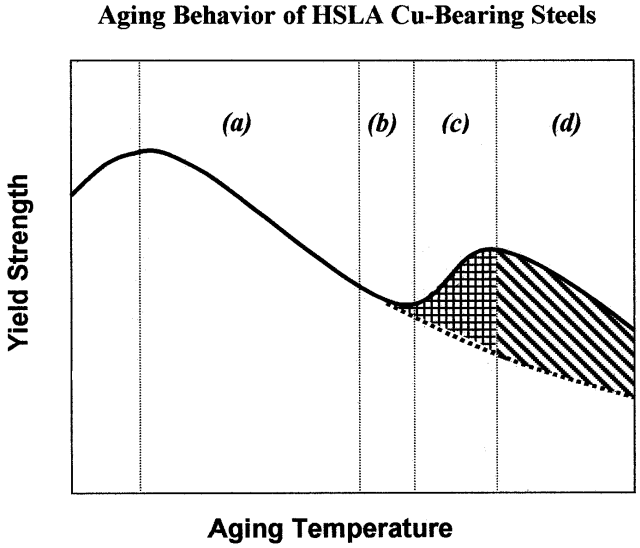

Fig. 16 Summary of the aging behavior of HSLA copper-bearing steels. (a) Recovery of matrix along with precipitation of Cu-particles. (b) New austenite formation. (c) New austenite transform to martensite. (d) New austenite transform predominately to Bainite.

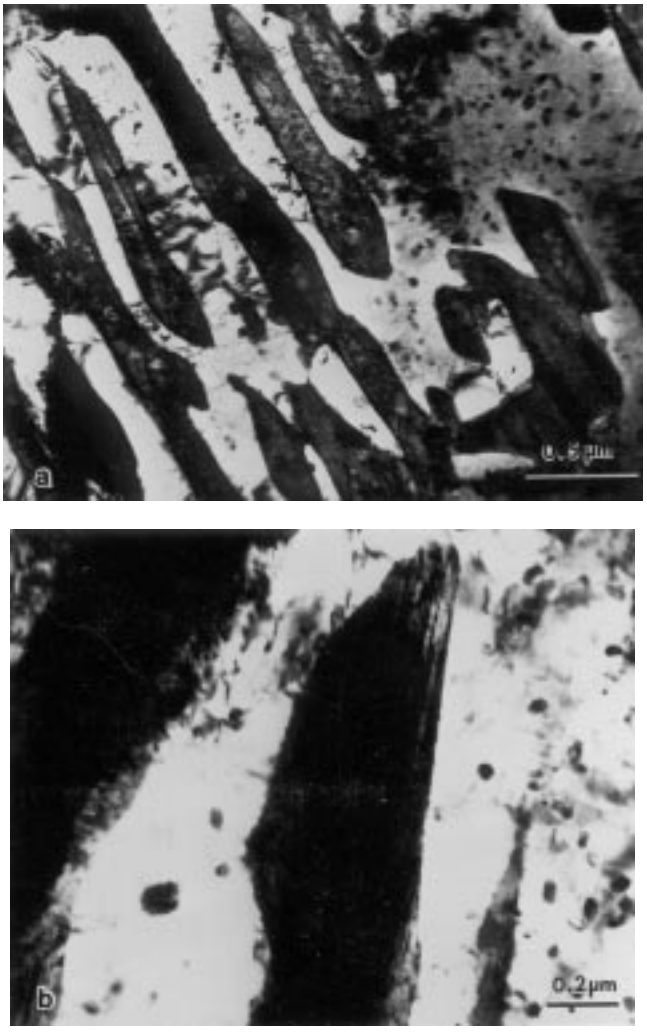

Fig. 15 TEM micrographs of steel B (aged at 708 °C). (a) New austenite transformed to martensite and retained austenite. (b) Evidence of microtwins formed in one of the martensite laths

(Ref 25) that this kind of structure possesses good impact toughness. The steels showed poor notch toughness at the peak strength levels (stage I of aging). This can be attributed to the additional matrix strengthening by a fine dispersion of copper particles and by impurity segregation to the grain boundaries.

In stages II and III of aging (above 600 °C), the steels showed a remarkable improvement in resistance to ductile as well as brittle fracture. As described earlier, the coarsening of copper precipitates, recovery and partial recrystallization of the lath structure, and the formation of a highly stable new austenite characterizes stage II. The improvement in toughness in this stage may partly be due to the fact that the new austenite acts as a sink for detrimental grain boundary impurities and thus reduces intergranular fracture, which is in accordance with earlier work (Ref 26, 27). Furthermore, other studies (Ref 28, 29) have shown that the major source of toughening is due to the gettering of carbon from the martensite matrix through its segregation to the new austenite. The secondary strengthening occurring in stage III of aging does not have a large effect on the toughness of the steel. The excellent toughness effect is due to the additional refinement of the microstructure due to the formation of new austenite islands. Also, these islands of retained new austenite present additional barriers to the growth of cleavage cracks.

4.3 Role of Copper on the Structure and Properties

The contribution of copper to the microstructure and mechanical properties of HSLA-100 steels can be summarized as follows:

- When in solution in austenite at 900 °C, copper will act to lower the transformation temperature (M_s or B_s) upon quenching. This will lead to an overall increase in strength at all aging conditions.
- When in the form of precipitates, copper will contribute to the overall strength by precipitation hardening when aged near 450 °C. The copper precipitates retard the recovery and recrystallization of the as-quenched matrix. This will also lead to higher strength levels at all aging conditions.
- As the aging temperature increases, the amount of copper in solution in the new austenite also increases. This acts to lower the Ac_1 and leads to the formation of new austenite at lower aging temperatures. Thus, austenite begins to form in matrix structures of higher strength levels.
- The sharp increase in low-temperature notch toughness observed with increasing aging temperature correlates with the presence of the new austenite formed at the aging temperature.
- The extent of the increase in toughness caused by the new austenite is directly related to its local composition at the aging temperature. For example, very rich new austenite that formed at aging temperatures close to the Ac_1 was very stable and did not transform during the air cooling to room temperature. This led to the highest level of toughness observed. As the aging temperature increased and the amount of the new austenite increased, its average chemical composition decreased. This austenite can transform during cooling, and the resulting structures depend on the exact composition and hardenability. As the aging temperature and the amount of the new austenite further increases, the composition of the austenite decreases with an accompanying decrease in hardenability. Hence, the products of transformation of this new austenite will change with its hardenability, e.g., from martensite to bainite as the aging temperature increases from 708 to 720 °C.
- The transformation characteristics of the new austenite formed during aging is, of course, a function of its complete composition and not only of copper itself.
- The retardation of recovery and recrystallization, together with the formation of stable austenite at low temperatures, give an aged structure an excellent combination of strength and low-temperature notch toughness.

5. Conclusions

- Copper precipitation-strengthened steels can exhibit an excellent combination of high strength and high resistance to low-temperature fracture.
- HSLA-100 steels show a typical aging behavior. The maximum strength is achieved at an aging temperature of 450 °C. The resistance to low-temperature fracture is very low at the peak strength levels. The impact toughness improves as the aging temperature increases.
- The best combination of strength and toughness is obtained when the steel is aged at approximately 640 °C.
- The extraordinary improvement in toughness at 640 to 665 °C is associated with the formation of a highly alloyed, thermally stable austenite formed at the lath boundaries. The new austenite is found to be rich in alloying elements such as nickel, copper, manganese, and chromium.
- The increase in strength at aging temperatures above 665 °C is due to the formation of a higher volume fraction of austenite and its subsequent transformation to martensite on air cooling.
- In general, the major factors that contribute to the strength and toughness characteristics of HSLA-100 steels in the aged condition are the partially recrystallized matrix, the uniform distribution of copper precipitates, the uniform distribution of Nb(C, N) particles, and the presence of the new austenite.

References

1. T.W. Montemarano, B.P. Sack, M.G. Vassilaros, and H.H. Vanderveldt, *J. Ship. Prod.*, Vol 2 (No. 3), Aug 1986, p 145
2. T.L. Anderson, J.A. Hyatt, and J.C. West, *Weld. J.*, Sept 1987, p 21
3. A.D. Wilson, "*High Strength Weldable A710 Type Steels*," Lukens Steel Co., Coatesville, PA, June 1986
4. B.A. Graville, *Welding of HSLA (Microalloyed) Structural Steels: Proc. Int. Conf.*, A.B. Rothwell and J.M. Gray, Ed., American Society for Metals, 1978, p 85
5. T. Haze and S. Achara, in *Proc. Seventh Int. Conf. Offshore Mechanics and Arctic Engineering, 7-12 Feb 1988, Houston, TX*, ASME, New York
6. F.B. Pickering, *High Strength Low-Alloy Steels—A Decade of Progress*, Union Carbide Corp., New York, 1977, p 9
7. C.I. Garcia and A.J. DeArdo, *Proc. World Materials Congress 1988: Microalloyed HSLA Steels*, ASM International, 1988, p 291
8. O. Kubaschewski, *Iron Binary Phase Diagrams*, Springer-Verlag/Heidelberg and Verlag Stahleisen mbH, Dusseldorf, 1982

9. I. LeMay and M.R. Krishnadev, *Copper in Iron and Steel*, I. LeMay and L.M. Schetky, Ed., John Wiley & Sons, 1982, p 5
10. R.W.K. Honeycombe, *Steels: Microstructure and Properties*, American Society for Metals, 1982, p 76
11. E. Hornbogen and R.C. Glenn, *Trans. Met. Soc. AIME*, Vol 218, 1960, p 1064
12. E. Hornbogen, *Acta Metall.*, Vol 10, 1962, p 525
13. E. Hornbogen, *Trans. ASM*, Vol 57, 1964, p 120
14. S.R. Goodman, S.S. Brenner, and J.R. Low, Jr., *Metall. Trans.*, Vol 4A, 1973, p 2363
15. S.R. Goodman, S.S. Brenner, and J.R. Low, Jr., *Metall. Trans.*, Vol 4A, 1973, p 2371
16. G.R. Speich and R.A. Oriani, *Trans. Met. Soc. AIME*, Vol 233, April, 1965, p 623
17. R.A. Ricks, P.R. Howell, and R.W.K. Honeycombe, *Metall. Trans.*, Vol 10A, Aug 1979, p 1049
18. C.I. Garcia and A.J. DeArdo, *Metall., Trans.*, Vol 12A, March 1981, p 521
19. D. Turnbull, *Atom Movements*, American Society for Metals, 1951, p 129
20. P.G. Shewmon, *Diffusion in Solids*, McGraw-Hill, 1963, p 172
21. J.I. Kim, H.J. Kim, and J.W. Morris, Jr., *Metall. Trans.*, Vol 15A, Dec 1984, p 2213
22. Y.H. Kim, H.J. Kim, and J.W. Morris, Jr., *Metall. Trans.*, Vol 17A, July 1986, p 1157
23. W. Steven and A.G. Haynes, *Journal of Iron and Steel Institute*, Vol 183, 1956, p 349
24. K.C. Russell and L.M. Brown, *Acta Metall.*, Vol 20, July 1972, p 969
25. G. Thomas, The Physical Metallurgy and Alloy Design of Dual Phase Steels, *Frontiers in Materials Technologies*, M.A. Meyers and O.T. Inal, Ed., Elsevier Science Publishers B.V., Amsterdam, 1985, p 89
26. C.W. Marshall, R.H. Hehemann, and A.R. Troiano, *Trans. ASM*, Vol 55, 1962, p 135
27. J. Kim and J.W. Morris, Jr., *Metall. Trans.*, Vol 11A, 1980, p 1401
28. D. Frear and J.W. Morris, Jr., *Metall. Trans.*, Vol 17A, Feb 1986, p 243
29. J.I. Kim, C.K. Syn, and J.W. Morris, Jr., *Metall. Trans.*, Vol 14A, Jan 1983, p 93